SCIENCE CHINA
Information Sciences

• MOOP •

October 2018, Vol. 61 104201:1–104201:3
https://doi.org/10.1007/s11432-017-9476-y

A simulator with an elastic guidewire and vascular system for minimally invasive vascular surgery

Xiaoran CHENG[1], Xiaoliang XIE[1,2], Guibin BIAN[1], Zengguang HOU[1,2,3*], Shiqi LIU[1] & Zhanjie GAO[1]

[1]*State Key Laboratory of Management and Control for Complex Systems, Institute of Automation, Chinese Academy of Sciences, Beijing* 100190*, China;*
[2]*University of Chinese Academy of Sciences, Beijing* 100049*, China;*
[3]*CAS Center for Excellence in Brain Science and Intelligence Technology, Beijing* 100190*, China*

Received 7 December 2017/Revised 4 April 2018/Accepted 1 June 2018/Published online 21 August 2018

Citation Cheng X R, Xie X L, Bian G B, et al. A simulator with an elastic guidewire and vascular system for minimally invasive vascular surgery. Sci China Inf Sci, 2018, 61(10): 104201, https://doi.org/10.1007/s11432-017-9476-y

Simulators play an important role in minimally invasive vascular surgery training. A challenging task for the simulator is to model an elastic guidewire and an elastic vascular system, both of which are important aspects for vascular surgery. However, many simulators treat the virtual vascular system as a rigid object, which reduces the immersion of operators. In this study, a virtual guidewire is first modeled based on Cosserat rod theory. Second, the stretching and bending constraints are introduced into the mass-spring vascular model according to the conservation of linear and angular momentum, making the model more stable and the deformation of blood vessels more realistic. Furthermore, the traditional dihedral angle constraint is replaced by our new bending constraint, which simplifies the complexity of the calculation. Finally, some experiments are conducted to demonstrate the effectiveness and accuracy of our vascular and guidewire models.

Introduction. Simulators based on virtual reality are becoming continually more popular in the medical training domain. Furthermore, a training simulator for minimally invasive vascular surgery, which is an effective aid for treating coronary heart disease, can overcome many drawbacks of traditional training methods. The modeling of deformable objects presents a challenging task for such a training system. Zhang et al. [1] proposed a layered rhombus chain-connected haptic deformation model, and later in [2] a non-uniform regularizer was applied to perform the deformation smoothly. Sharei et al. [3] reviewed computer-based models in surgery training systems, and emphasized the importance of the deformation of the vascular system in the training system. However, this is not considered in many studies. In [4], virtual surgery based on rigid vascular and elastic guidewire models was introduced. In order to increase the immersion of doctors, an elastic mass-spring-based vascular model is proposed in this paper. Wang et al. [5] developed a method to identify the spring coefficient in a mass-spring model, and proved that the coefficient of elasticity is related to the radius of the blood vessel. In the original mass-spring model, a virtual spring with linear elasticity is assumed. However, this may result in a large deformation. Duan et al. [6] introduced new constraints to improve the accuracy of the deformation. In this study, we apply a length constraint and a new angular constraint to our mass-spring vascular model.

Physical model. An overview of our simulator is presented in Figure 1(a). The guidewire and vas-

* Corresponding author (email: zengguang.hou@ia.ac.cn)

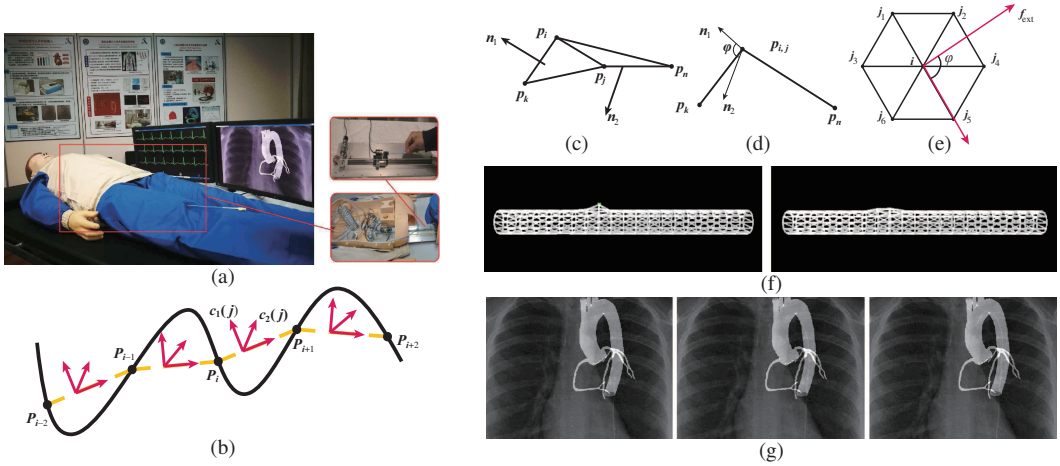

Constraint type	Iterations	Constraint numbers	Responding time (s)
The dihedral angle constraint	1000	629	23.1781
New bending constraint	1000	629	41.6689

(h)

Figure 1 (Color online) (a) Overview of the system; (b) the guidewire model based on Cosserat rod theory; (c) dihedral angle constraint; (d) simplified dihedral angle constraint; (e) modified constraint; (f) the deformation before and after the stretching and the bending constraint are added; (g) interface of minimally invasive vascular surgical training system; (h) comparison of the responding time between old and new constraints.

cular models will be respectively discussed in the following sections.

Guidewire model. A guidewire model based on Cosserat rod theory can be introduced as shown Figure 1(b), where N spatial control points $\boldsymbol{P}_i$, $i \in [1, N]$ are included. There exist right-handed Cartesian coordinates $(\boldsymbol{c}_1(j), \boldsymbol{c}_2(j), \boldsymbol{c}_3(j))$, $j \in [1, N-1]$, which are used to calculate the penalty energy. Furthermore, $\boldsymbol{c}_3$ is a unit vector parallel to $\boldsymbol{P}'$, which is equal to $(\boldsymbol{P}_{i+1} - \boldsymbol{P}_i)$.

There are three types of energy in Cosserat rod theory, namely, the elastic potential EP_e, the dissipation energy D_e, and the constraint C_e [7]. The inner torques and forces [4] can be calculated as follows:

$$\boldsymbol{T}_{\mathrm{in}} + \boldsymbol{F}_{\mathrm{in}} = -\frac{\partial(\mathrm{EP}_e^b + C_e)}{\partial \boldsymbol{\eta}_q} - \frac{\partial D_e^r}{\partial \dot{\boldsymbol{\eta}}_q} - \frac{\partial(C_e)}{\partial \boldsymbol{\eta}_p} - \frac{\partial D_e^t}{\partial \dot{\boldsymbol{\eta}}_p},$$

where $\boldsymbol{\eta}_p$ and $\boldsymbol{\eta}_q$ denote the positions of the N control points and $N-1$ unit quaternions, respectively; EP_e^b is used to measure the bending and torsional deformation of the guidewire; D_e^r denotes how much energy is required to bring the two shapes into alignment; and D_e^t represents the energy loss owing to internal friction. Then, the evolution of the control points can be described in the following form:

$$\boldsymbol{M}_p \ddot{\boldsymbol{\eta}}_p = \boldsymbol{F}_{\mathrm{in}} + \boldsymbol{F}_{\mathrm{ext}} + \boldsymbol{F}_{\mathrm{in}}^{\mathrm{ine}},$$

where $\boldsymbol{F}_{\mathrm{in}}^{\mathrm{ine}}$ [4] is the force produced by the constraint, which represents the inextensibility of $(\boldsymbol{P}_{i+1} - \boldsymbol{P}_i)$, and the constraint can be described as

$$C_{\mathrm{ine}}[i] := (\boldsymbol{P}_{i+1} - \boldsymbol{P}_i) \cdot (\boldsymbol{P}_{i+1} - \boldsymbol{P}_i) - |\boldsymbol{P}_{i+1}^0 - \boldsymbol{P}_i^0|^2 = 0.$$

Further details can be found in [4].

Vascular model. In the simulator, we employ the improved mass-spring theory to simulate the behavior of the vascular model, which has a single-layered surface structure.

The model includes N_1 spatial points. Let us denote the mass of point i by m_i, and the point following i by j. We assume that the mass is evenly distributed on the surface of a blood vessel. A virtual spring is added between points i and j. The force exerted on any point $i \in [1, N_1]$ can be expressed by $\boldsymbol{f}_i$, which includes $\boldsymbol{f}_{\mathrm{ext}}$ and $\boldsymbol{f}_{\mathrm{in}}$. We denote the position matrix by $\boldsymbol{x} \in \boldsymbol{R}^{3N_1}$, and the force matrix by $\boldsymbol{f} \in \boldsymbol{R}^{3N_1} := \boldsymbol{f}_{\mathrm{in}} + \boldsymbol{f}_{\mathrm{ext}}$. The evolution of any point can be calculated according to Newton's second law:

$$\boldsymbol{M}\ddot{\boldsymbol{x}} = \boldsymbol{f}.$$

Furthermore, we use the Euler integrator to update the positions of points.

In order to improve the simulation accuracy, we introduce position-based dynamics to determine a suitable $\Delta \boldsymbol{p}$ subject to $C(\boldsymbol{p} + \Delta \boldsymbol{p}) = 0$. Furthermore, we employ the binomial expansion of the Taylor series to express the constraint as

$$C(\boldsymbol{p} + \Delta \boldsymbol{p}) \approx C(\boldsymbol{p}) + \nabla \boldsymbol{p} C(\boldsymbol{p}) \cdot \Delta \boldsymbol{p} = 0.$$

Here, we always keep the direction of $\Delta \boldsymbol{p}$ consistent with $\boldsymbol{p}$, as follows:

$$\Delta \boldsymbol{p} = k \nabla \boldsymbol{p} C(\boldsymbol{p}). \tag{1}$$

Then, we eliminate the middle variable k,

$$\Delta \boldsymbol{p} = -\frac{C(\boldsymbol{p})}{|\nabla \boldsymbol{p} C(\boldsymbol{p})|^2} \nabla \boldsymbol{p} C(\boldsymbol{p}). \tag{2}$$

Typical constraints include the stretching constraint, which is used to maintain the length invariance of each edge, and the bending constraint, which is used to maintain the dihedral angle invariance of each pair of adjacent triangles.

• Stretching constraint. For any spring, there exists a vector $\boldsymbol{p} = (\boldsymbol{p}_i^{\mathrm{T}}, \boldsymbol{p}_j^{\mathrm{T}})^{\mathrm{T}}$, where $\boldsymbol{p}_i^0$ and $\boldsymbol{p}_j^0$ denote the initial positions of points i and j, respectively. The stretching constraint is

$$C_{\mathrm{len}}(\boldsymbol{p}) = |\boldsymbol{p}_i - \boldsymbol{p}_j| - |\boldsymbol{p}_i^0 - \boldsymbol{p}_j^0| = 0.$$

From (1) and (2), we can obtain $\Delta \boldsymbol{p}_i = -\Delta \boldsymbol{p}_j$ as

$$\Delta \boldsymbol{p}_i = -\frac{|\boldsymbol{p}_i - \boldsymbol{p}_j| - |\boldsymbol{p}_i^0 - \boldsymbol{p}_j^0|}{2} \cdot \frac{\boldsymbol{p}_i - \boldsymbol{p}_j}{|\boldsymbol{p}_i - \boldsymbol{p}_j|}.$$

• Bending constraint. In traditional methods, the dihedral angle constraint is employed to correct the bending degrees of objects. Here, $\boldsymbol{p} = (\boldsymbol{p}_i^{\mathrm{T}}, \boldsymbol{p}_j^{\mathrm{T}}, \boldsymbol{p}_k^{\mathrm{T}}, \boldsymbol{p}_n^{\mathrm{T}})^{\mathrm{T}}$ is a vector denoting the positions of the four points of each dihedral angle element. We can express this constraint as follows:

$$C_{\mathrm{dih}}(\boldsymbol{p}) = \mathrm{acos}\left(\frac{\boldsymbol{n}_1 \cdot \boldsymbol{n}_2}{|\boldsymbol{n}_1||\boldsymbol{n}_2|}\right) - \varphi_0' = 0.$$

Here, $\boldsymbol{n}_1 := (\boldsymbol{p}_j - \boldsymbol{p}_i) \times (\boldsymbol{p}_k - \boldsymbol{p}_i)$ and $\boldsymbol{n}_2 := (\boldsymbol{p}_j - \boldsymbol{p}_i) \times (\boldsymbol{p}_n - \boldsymbol{p}_i)$ denote the normal vectors of the triangles formed by the points (i, j, k) and (i, j, n), respectively, and φ_0' is the initial dihedral angle.

Considering the complexity of computing $\Delta \boldsymbol{p}$ according to the dihedral angle constraint in Figure 1(c) and (d), we aim to determine a new constraint to replace this one. As shown in Figure 1(e), the variation of the angle between $\boldsymbol{f}_{\mathrm{ext}}$ and the line (i_1, j_1) represents the bending degree of each edge, and we can calculate $\Delta \boldsymbol{p}$ according to the varied $\boldsymbol{f}_{\mathrm{ext}}$.

$$C_{\mathrm{angle}}(\boldsymbol{p}) = \mathrm{acos}\left(\frac{(\boldsymbol{p}_{i_1} - \boldsymbol{p}_{j_1}) \cdot \boldsymbol{f}_{\mathrm{ext}}}{|\boldsymbol{p}_{i_1} - \boldsymbol{p}_{j_1}||\boldsymbol{f}_{\mathrm{ext}}|}\right) - \varphi_0 = 0.$$

Here, $\boldsymbol{p} = (\boldsymbol{p}_{i_1}^{\mathrm{T}}, \boldsymbol{p}_{j_1}^{\mathrm{T}})^{\mathrm{T}}$, and φ_0 is the original angle between $\boldsymbol{f}_{\mathrm{ext}}$ and the line (i_1, j_1).

Then, $\Delta \boldsymbol{p}_{j_1} = -\Delta \boldsymbol{p}_{i_1}$, and we denote $|\boldsymbol{p}_{i_1} - \boldsymbol{p}_{j_1}||\boldsymbol{f}_{\mathrm{ext}}| = a$ and $(\boldsymbol{p}_{i_1} - \boldsymbol{p}_{j_1}) \cdot \boldsymbol{f}_{\mathrm{ext}} = b$,

$$\Delta \boldsymbol{p}_{i_1} = \frac{\mathrm{acos}\frac{b}{a} - \varphi_0}{2\sqrt{a^2 - b^2}} [|\boldsymbol{p}_{i_1} - \boldsymbol{p}_{j_1}|^2 \boldsymbol{f}_{\mathrm{ext}} - b(\boldsymbol{p}_{i_1} - \boldsymbol{p}_{j_1})].$$

Experiments. In order to verify the effectiveness of our method, two experiments were conducted on a PC equipped with a 3.1 GHz Intel Core i5-2400 CPU and 8 GB RAM. Figure 1(f) shows the deformation when we apply the same instantaneous force at the same particle of two virtual pipes, which have the same geometry and different physical models. We can see that the deformation is smoother when the new constraints are employed in our physical model. In the second experiment shown in Figure 1(h), we calculate the time required for our program to iterate 1000 times. Comparing these two sets of data, we can observe a reduction in the time consumption when the dihedral angle constraint is replaced by our proposed bending constraint. Based on our virtual guidewire and vascular system, we simulate the intervention procedure. The results are illustrated in Figure 1(g). The guidewire passes through the large curvature of our virtual vascular system successfully. Thus, the stability of our models has been demonstrated.

Acknowledgements This work is partially supported by National Natural Science Foundation of China (Grant Nos. 61533016, U1613210, 61421004), and National High-tech Research and Development Program (Grant Nos. 2015AA042306, 2017YFC0110804, 2017YFE0112200).

Supporting information Videos and other supplemental documents. The supporting information is available online at info.scichina.com and link.springer.com. The supporting materials are published as submitted, without typesetting or editing. The responsibility for scientific accuracy and content remains entirely with the authors.

References

1 Zhang X R, Sun W, Song A G. Layered rhombus-chain-connected model for real-time haptic rendering. Artif Intel Rev, 2014, 41: 49–65
2 Zhu L F, Li W, Zhang X R, et al. Diffusion-based non-uniform regularization for variational shape deformation. Comput-Aided Des, 2016, 81: 61–69
3 Sharei H, Alderliesten T, van den Dobbelsteen J J, et al. Navigation of guidewires and catheters in the body during intervention procedures: a review of computer-based models. J Med Imag, 2018, 5: 010902
4 Cheng X R, Song Q K, Xie X L, et al. A fast and stable guidewire model for minimally invasive vascular surgery based on Lagrange multipliers. In: Proceedings of IEEE International Conference on Information Science and Technology, Vietnam, 2017. 109–114
5 Wang Y, Guo S X, Gao B F. Vascular elasticity determined mass-spring model for virtual reality simulators. Int J Mech Autom, 2015, 5: 1–10
6 Duan Y P, Huang W M, Chang H B, et al. Volume preserved mass-spring model with novel constraints for soft tissue deformation. IEEE J Biomed Health Inf, 2016, 20: 268–280
7 Spillmann J, Teschner M. CORDE: Cosserat rod elements for the dynamic simulation of one-dimensional elastic objects. In: Proceedings of Symposium on Computer Animation, San Diego, 2007. 63–72